Mapping burn severity and uncovering spread patterns of the 2021 Varibopi wildfire

Palaiologou Palaiologos[1,*], *Pantera* Anastasia[1], *Zianis* Dimitrios[1], *Papadopoulos* Andreas[1], and *Zografakis* Stavros[2]

[1]Agricultural University of Athens, Department of Forestry and Natural Environment Management, 36100, Karpenisi, Greece
[2]Agricultural University of Athens, Department of Agricultural Economics and Rural Development, 11855, Athens, Greece

Abstract. This work unveils how the wildfire of August 3rd, 2021 that initiated at the northeastern part of Attica (Varibopi), spread and burned during the four days of its active propagation. This fire is a characteristic large-scale event that affected the wildland-urban interface of Athens, revealing weaknesses of both pillars of fire management: prevention and suppression. Initially, we provide a short description of how and under which conditions (vegetation and weather) the fire initiated and propagated after debriefing reports, news articles and satellite data. Then, we applied the difference Normalized Burn Ratio on a pair of Sentinel 2A satellite images (one right before and another taken one year later) to map the extended burn severity and delineate the fire perimeter. Finally, using the Minimum Travel Time Algorithm, we simulated major spread vectors and rate of spread to answer how the fire would have been evolved in the absence of active fire suppression. We found that from the 8,445-ha included in the final delineated perimeter, 1,000 ha were unburned, 4,715 ha experienced low or moderate-low burn severity, and 2,730 moderate-high or high burn severity. Without suppression, the fire could have escaped from three directions to the west with high spread rate, potentially affecting the Parnitha National Park. The most imminent post-fire issue is not whether the conifer vegetation will recover, but if during the next decade vegetation management measures are not applied in selected locations, then a new ignition can spread faster and burn a more extended area compared to the 2021 fire.

1 Introduction

The ever-increasing frequency of large-scale fires (>10,000 hectares) in Greece is a matter of concern for civil protection and nature conservation agencies. The rugged topography of Greece is covered by diverse ecosystems with dense vegetation, usually surrounded by areas of residential development and human activities. The intensity and frequency of these activities near natural areas means that even small fires can have a significant negative impact. After the 2018 fires in Mati, when 102 died from a relatively small-sized incident, and the 2021 mega-fire in Evia (mega-fires are those that burned >40,000 ha), Greece has entered a new era that signals that the old ways of suppression and fuel management are no longer adequate to confront fast-spreading events or mega-fires.

Previous studies have well documented the extreme fire behavior of wildfire over the Greek landscape. Athanasiou and Xanthopoulos [1] studied and recorded the behavior of 12 large fires in the summer of 2007 and observed that the maximum spread speed was 11.2 km/h, with an average value of 3.5 km/h. The same authors used 95 measurements of the actual spread rate of historical surface fires and recorded that in low and high shrublands (maquis) spread rates ranged between 7-9 km/h, in short shrubs (*Sarcopoterium spinosum*) up to 8 km/h and in low grasslands up to 15.6 km/h [2]. Finally, for the 2018 fire in eastern Attica (Mati) they recorded average spreading speeds of 2 km/h, with a maximum speed of 7.8 km/h [3].

The wildfire in Varibopi, Attica, started on August 3rd, 2021 at 13:22 in a dense pine forest (*Pinus halepensis*) under a high-voltage (150KV) tower from the creation of strong electrical arcs (Figure 1). During the first two hours of its spread (13:30 - 15:30), winds with average intensities of 2 - 4 Bf and gusts of up to 5 Bf were blowing in the area. The fire in Upper Varibopi was brought under partial control in the early hours of Thursday August 5th.

However, on the same day a new fire ignited in the area of Vasilika Parnithas and combined with the continuous rekindling of the previous fire in the same area (Upper Varibopi) it quickly escalated in size and intensity. Then, the fire extended to Afidnes and burned all the forested area around the town, reaching the Athens – Thessaloniki highway, which it crossed (shortly before 22:00 on the same day) through spotting resulted from active crown burning and continued to burn eastwards, heading towards Agios Stefanos, Lake Marathon and Kapandriti. The fire also extended to Malakasa and burned all the forested area around the town. In Agios Stefanos and Stamata, the fire destroyed dozens of homes and businesses while a plastics factory

* Corresponding author: palaiologou@aua.gr

near Agios Stefanos was also burnt. The last active outbreaks of the fire were extinguished at the noon of 7 August. More than 450 firefighters, 150 vehicles, the Mobile Operations Centre OLYMPOS, three helicopters and seven firefighting aircrafts operated during the suppression, assisted by 40 firefighters from Cyprus, the Hellenic Army with infantry units, the Hellenic Police, volunteer firefighters as well as water trucks and supporting heavy machinery and equipment.

Fig. 1. Typical fuel conditions of the ignition area.

This work examines and presents the results obtained from the spatial fire simulation model FlamMap that utilize the Minimum Travel Time algorithm to assess the risk of future wildfire spread within the burnt areas, based on current and estimated future fuel conditions.

2 Materials and Methods

2.1 Mapping burn severity and fire perimeter

With some exceptions, many signs of burn severity in the landscape are evident immediately after the fire is extinguished. These are related to the process by which the burning has occurred, the charring and consumption of live vegetation and dead fuel, ash, and to changes in the nature of the exposed mineral soil. The exceptions, however, are important. They relate to initial vegetation recovery and delayed mortality, which also contribute to the short-term severity of fire effects.

Often these factors may not become apparent until at least the next growing season, so it may take some time for a more complete assessment of the fire effects. Considering the above, there are two approaches to estimate burn severity. The Initial Assessment captures the most immediate fire effects on the biophysical parameters present at the time of the fire. By waiting until the following year, the burned vegetation has some time to recover and show additional responses indicative of the initial burning severity. Delayed mortality may also be evident, revealing that plants that were green immediately after the fire eventually died in the following growing season.

Extended Assessment is more useful for the final visualization and assessment of short-term first-order fire effects [4]. It could also better capture long-term ecological consequences, such as impacts on sensitive communities or species, or other risk factors such as erosion and future fire potential. Sentinel 2A satellite imagery was used to create the fire severity assessment map, applying the Extended Assessment. The satellite image pair covers the coupling dates of 3 August 2021 - 18 August 2022. The Normalized Burn Ratio (NBR) equation was applied to the satellite images to calculate the two indices (pre-fire NBR and post-fire NBR) in channels 8 (NIR) and 12 (SWIR) of Sentinel 2A [(Band 8 - Band 12) / (Band 8 + Band 12)].

The dNBR was then calculated using the equation dNBR = pre-fire NBR - post-fire NBR. The result obtained was multiplied by 1,000 to classify it into the seven burn severity classes based on the Key and Benson [4] categorization. Specifically, values of -500 to -251 were assigned to high regeneration, -250 to -101 to low regeneration, -100 to +99 to unburned, +100 to +305 to low severity, +306 to +439 to medium-low severity, +440 to +659 to medium-high severity, and finally, +660 to +1,300 to high burn severity.

2.2 Simulations of fire spread with the MTT algorithm

First, a simulation was performed with the MTT algorithm to assess how the historical fire of August 3rd 2021 evolved and behaved. This simulation is the control simulation, used for comparison with the corresponding simulations conducted with the vegetation conditions estimated to prevail in a) 2-3 years, b) 4-5 years, and c) 6-10 years, after the 2021 fire. The moisture conditions set were very dry for all fuel models (1-hr: 3%, 10-hr: 4%, 100-hr: 5%, Live Herbaceous: 30%, Live Woody: 60%), wind speed of 10 km/h at 10 m from the ground, predominant wind direction 45° with downslope winds blowing downhill, crown foliage moisture set to 100% (120% is an appropriate value for average mid-summer conditions and 100% value for dry conditions), and calculating crown fire spread with the Finney's [5] method. The ignition point was assigned to the location where the first ignition of the 2021 fire started, the probability of spotting was 0.05 with an ignition delay of two minutes, and a simulation duration was set to 5,000 minutes of active burning (3.5 days). Meteorological conditions remained unchanged throughout the simulation (i.e., no change in wind direction and intensity). The effect of ground and aerial firefighting was not simulated on any part of the fire front.

A set of four simulations were run with exactly the same parameters, with the only difference being the changes in the fuel models, as presented in Table 1, and with all crown parameter values (stand height, canopy base height, canopy base density, canopy cover) set to zero since the simulated fire is not expected to develop into a crown fire due to the low post-fire vegetation height. Burnt areas in Mediterranean low-elevation pine forests after about five years from the fire show a high density of regenerating trees in layers of different heights but with small diameter at breast height, that contain

large amounts of fuel, especially live foliage and small diameter branches (about 56 tonnes per hectare) (Figure 2 & Figures 11-12 in the discussion section).

In these areas there is a high horizontal continuity of vegetation, which is often complemented by the presence of tall shrubs mixed with annual vegetation (Figure 12). These areas are typically prone to extremely fast fire rate of spread. Other areas formerly dominated by *Pinus halepensis* forests are covered by low discontinuous shrubs and phrygana in the first 2-3 years after fire, sometimes in mixture with annual and herbaceous vegetation, and very low height conifer regeneration (<1 m) (Figure 11).

2.3 Stochastic fire simulations

In total, 10,000 fire events were simulated at a spatial resolution of 60 m, activating Finney's [5] method of calculating crown fires. Two simulations were conducted, one for vegetation/fuel conditions prevailing before the 2021 fire, and one for conditions expected to exist in the area ten years after the 2021 fire, i.e., for the year 2031 (Table 1). Both simulations had the same parameters (meteorological conditions, number and location of ignitions, etc.) so that any changes can be attributed to the changes that will occur due to modifications in the composition, structure and composition of the vegetation. All values of canopy parameters for 2031 were set to zero, as the fire is not expected to develop into a crown fire due to the low vegetation height.

For a better understanding of Table 1, the Fuel Model (FM) TU4 is assigned to regions with the features shown in Figure 2, FM GS2 to regions as depicted in Figure 11, and FM TU1 to regions as depicted in Figure 12. The simulated ignitions were placed on the landscape based on a spatial raster layer of ignition probabilities (with values 0 to 1) of the study area. The spatial grid was derived from historically recorded ignitions in the greater Attica region, specifically 735 recorded incidents with >0.1 ha burned area for the period 2004-2022, created using the Kernel Density Smoothing by defining a three-mile search radius.

Fig. 2. High-density regeneration of *Pinus halepensis* in stands in which some mature individuals of the species survived, six years after a fire.

The results are the production of one Burn Probability-BP map for each period, showing which areas are most vulnerable and predisposed to burn from one or more potential fire incidents, as well as which areas are more "non-burnable". The BP for each cell is an estimate of the probability that that cell will burn from a random ignition within the analysis area and with burning conditions similar to those of historical fires in the area. The map has a BP range from 0 (unburned) to 1 (maximum burn probability). Conditional Flame Length (Conditional Flame Length-CFL) is the weighted probability of the flame length, a metric that describes the intensity of the fire.

The MTT does not involve the estimation of the absolute risk of future fire occurrence, but it does provide a quantitative framework for analyzing the potential losses from specific fire events, while providing a method for quantifying the effectiveness of fuel management scenarios in the field by estimating the potential spread, intensity and impacts of fire.

Table 1. Changes in fuel models (FM) after the fire. The FM are from the set of 40 created by Scott and Burgan [6].

Years after fire	FM-Shrubs	FM-Conifers	Description
1	98	98	Non-burnable; Insufficient fuel quantity
2-3	GS2-122	TU1 - 161	Low discontinuous shrubs and phrygana mixed with annual and herbaceous vegetation - very low height conifer regeneration (<1 m). Shrubs: low density
4-5	SH2-142	GS2-122	Low-height Mediterranean scrub mixed with annual and herbaceous vegetation. Shrubs: denser. Annual vegetation: thinner from the first 2-3 years. Low-height coniferous regeneration (<2 m)
6-10	SH5 - 145	TU4 - 164	Medium-height Mediterranean scrub; medium-height coniferous regeneration (2-5 m)

3 Results

3.1 Burn severity and fire perimeter

Initially, the dNBR index was used to create a more valid comprehensive perimeter, which defines the outer boundaries of the fire but does not exalt the unburned enclaves. The perimeter was created by converting all the low to higher burn severity raster values to a polygon and then visually analyzing and digitizing to ensure that it accurately captures the outer boundaries. The final burned area is 8,444 ha, including the resulting spotting to the east on the north side of the Marathon Dam (19.5 ha).

The Extended Assessment of burn severity gives a much more diverse picture of what has happened in the region, with better separation between severity classes. This is because the Extended Assessment can capture both delayed mortality and survival of species e.g., plants that had scorched leaves, shed them and new green ones emerged. The analysis showed (Figure 3) that

12% of the site was classified as unburned (990 ha) and almost 30% burned with low severity (2,465 ha). High severity burned portions of the area comprised <1% of the total burned area (50 ha), and 32% was classified as medium-high severity (2,680 ha), while 27% was classified as medium-low severity (2,250 ha).

In conclusion, the high priority areas to receive additional restoration measures, including the monitoring of regeneration success, are the areas with medium-high severity, followed by areas with medium-low severity. Overall, the 60% of the burned area may have already experienced or will experience some negative effects from the fire in the future. These results can be used to design field inventories to assess the success of natural regeneration, in combination with other geophysical and vegetation data (slope, soil parameters and composition, abundance and structure of the post-fire plant community).

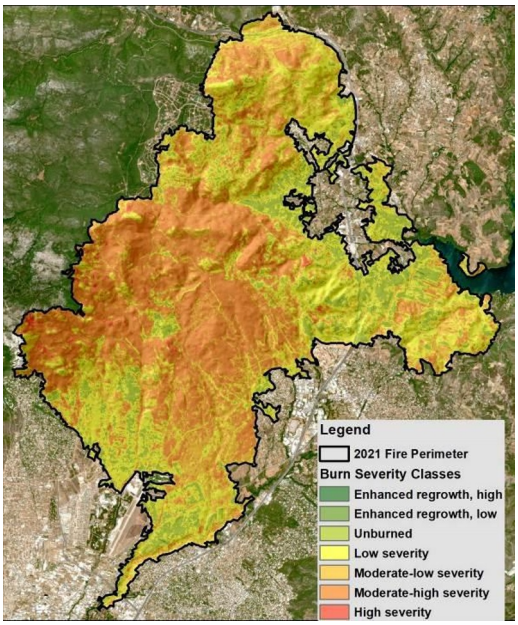

Fig. 3. Extended burn severity assessment, as calculated with the dNBR index applied to Sentinel 2A satellite images.

3.2 Major fire flow paths

By calculating the major flows paths of fire spread across the landscape, we can identify the directions in which a fire is expected to move without worrying about how it will be affected by suppression efforts or the likely duration of specific wind speeds. The major flow paths allow us to search for opportunities to contain them by either proactively creating firebreaks or fuel management projects, and by better planning suppression operations so that aerial firefighting or the application of backfires are carried out where they have the greatest chances of producing a favorable outcome. An attempt was made to mark the flows from similar directions in the same color to make it easier to compare them.

From the basic simulation (Figure 4) we see that flow #1 (yellow) was the one that burned in the eastern part of the fire and to the north, in a direction parallel to the highway, flow #2 (grey) was the main flow path and the one that burned the central part, flow #3 (red) was the one that burned south towards Kifissia, while flow #10 (fuchsia) went eastwards and stopped at the highway without extending further. Finally, flow #4 (light green) burned the western and northwestern portions of the 2021 fire. All five of these flows are distinct in the four simulations, but with different extents of expansion. In particular, differences are found in the simulation for the 4-5 years after the fire (Figure 6), where flow #1 does not expand significantly and flow #4 was merged into flow #2. In the three other cases (Figures 4, 5 & 7), the main flows #1 and #2 (that burned nearly half of the burned area of 2021) started on the same branch and crossed west of Cryoneri. There, a significant opportunity arises to stop future fires from a northward expansion. In all simulations, we see that it was not possible to simulate the spotting fire on the east side of the highway that expanded and burned on the southern and western shores of the Marathon Dam.

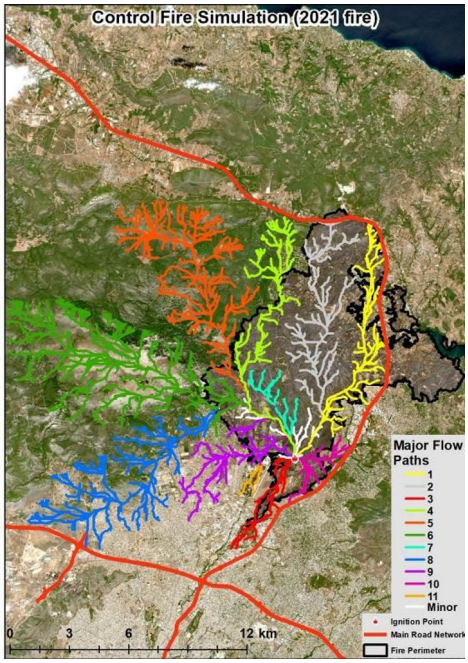

Fig. 4. Major fire flow paths for the fuel conditions that existed during the 2021 wildfire.

Another important branch is the one heading northwest (flow #7 - cyan) which branches off with other flows that have the potential to drive the fire with momentum to the west (flows #6 - green, #5-orange and #8-blue). The later three branched did not occur on the 2021 fire either due to suppression, or due to changing weather conditions (winds blew westerly after the first day quite frequently).

Specifically, the simulations showed that flow #5 is directed to the northwest and burns the northern fringes of Parnitha, flow #6 passes the top of Parnitha and enters the burned area of 2007, while flow #8 is directed towards Fili, on the southern fringes of Parnitha. It is understood that if the fire did eventually manage to enter these areas, especially the burnt areas of 2007, the ecological destruction of the area would be irreversible.

Another hazardous flow is #9 (purple), which enters the northern parts of Acharnon and the Thracomacedones (suppressed in 2021) (see Figure 5 & 6). In all simulations, flow #9 is quite active and due to the characteristics of the settlements in the area (Intermix WUI with coniferous vegetation in Thracomacedones and short shrubs with annual vegetation north of Acharnes), there is a very high vulnerability in the buildings of the area and exposure of a large part of their population. In Figure 7, we see that flow #9 is well-established and expanded, burning all the southern slopes of Parnitha and burning through the WUI.

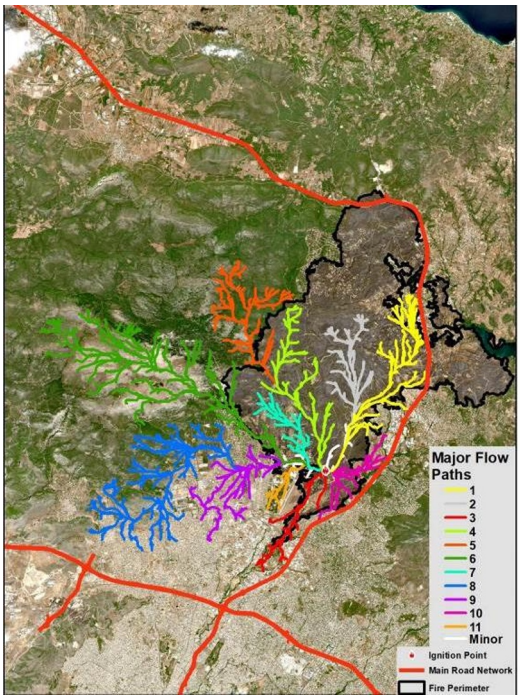

Fig. 5. Major fire flow paths for the fuel conditions expected to prevail 2-3 years after the fire.

By comparing the results of the simulations with respect to the propagation speed (rate of spread) (Figure 8) and fireline intensity (Figure 9) of the fire front, and from the visual assessment of the spreading fluxes, we found that up to the sixth year after the fire, no extreme fire behavior is expected and the only emphasis that should be given is to prevent a possible fire from escaping towards Parnitha. For the period 6-10 years after the fire, the results revealed the enlargement of the total burnt area, the spreading flows directed towards all sides of Parnitha were much more intense, while the fire behavior within the burnt area in 2021 no longer shows significant differences, on the contrary, in large parts of the area the rate of spread and the fireline intensity of the fire front are much higher than in 2021 (Figures 8-9 & Table 2). We can notice how both fire rate of spread (Figure 8) and fireline intensity (Figure 9) increase over the years after 2021, where warmer colors depict an increase and cooler colors depict a decrease compared to the control simulation of the 2021 fire.

Table 2. Comparable table of the area (%) that experienced increase (negative values), remained relatively stable (values close to zero) and decreased (positive values) compared to the control conditions for rate of spread and fireline intensity.

Years after fire	Rate of Spread Class (m/min)	Fireline Intensity Class (kW/m)	Rate of Spread (%)	Fireline Intensity (%)
2-3	-16.5 to -3	-6,397 to -60	0.2%	2%
	-3 to -0.5	-60 to 250	2.8%	33%
	-0.5 to 15	250 to 14,326	97%	65%
4-5	-16.5 to -3	-6,397 to -60	2%	6%
	-3 to -0.5	-60 to 250	18%	45%
	-0.5 to 15	250 to 14,326	80%	49%
6-10	-16.5 to -3	-6,397 to -60	16%	41%
	-3 to -0.5	-60 to 250	24%	49%
	-0.5 to 15	250 to 14,326	60%	10%

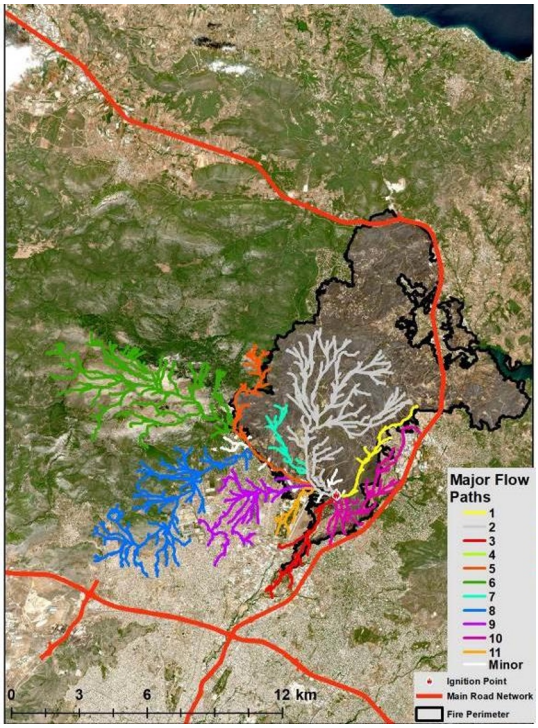

Fig. 6. Major fire flow paths for the fuel conditions expected to prevail 4-5 years after the fire.

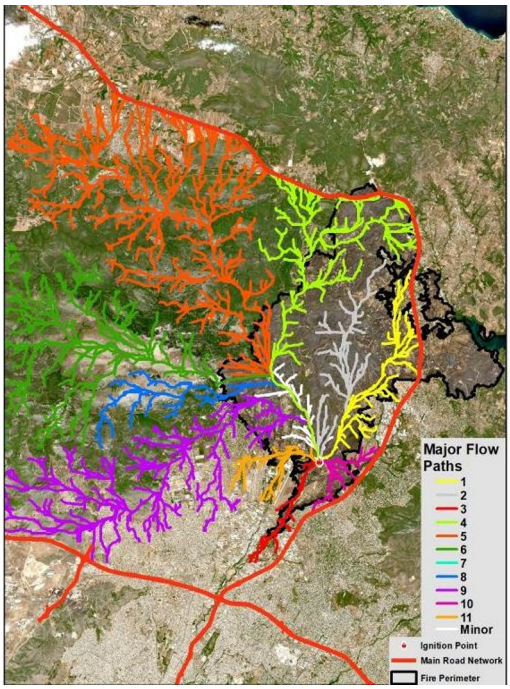

Fig. 7. Major fire flow paths for the fuel conditions expected to prevail 6-10 years after the fire.

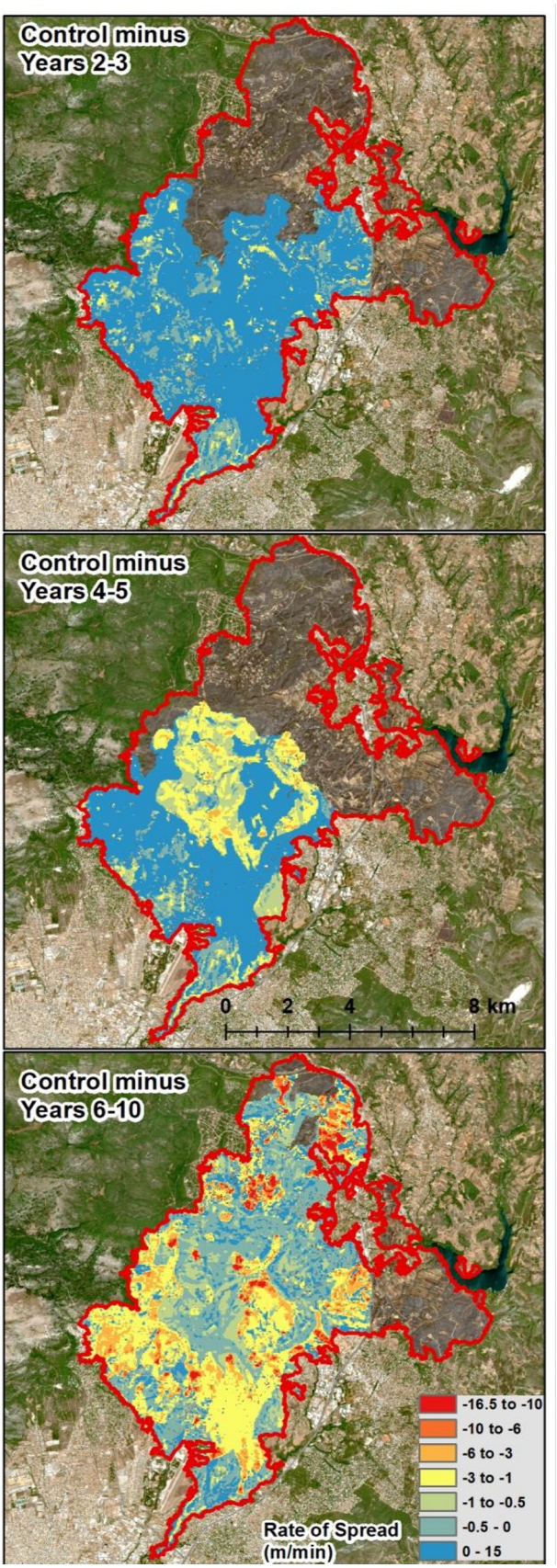

Fig. 8. Differences in rate of spread (m/min) after subtracting from the control simulation the results for the years 2-3, 4-5 and 6-10.

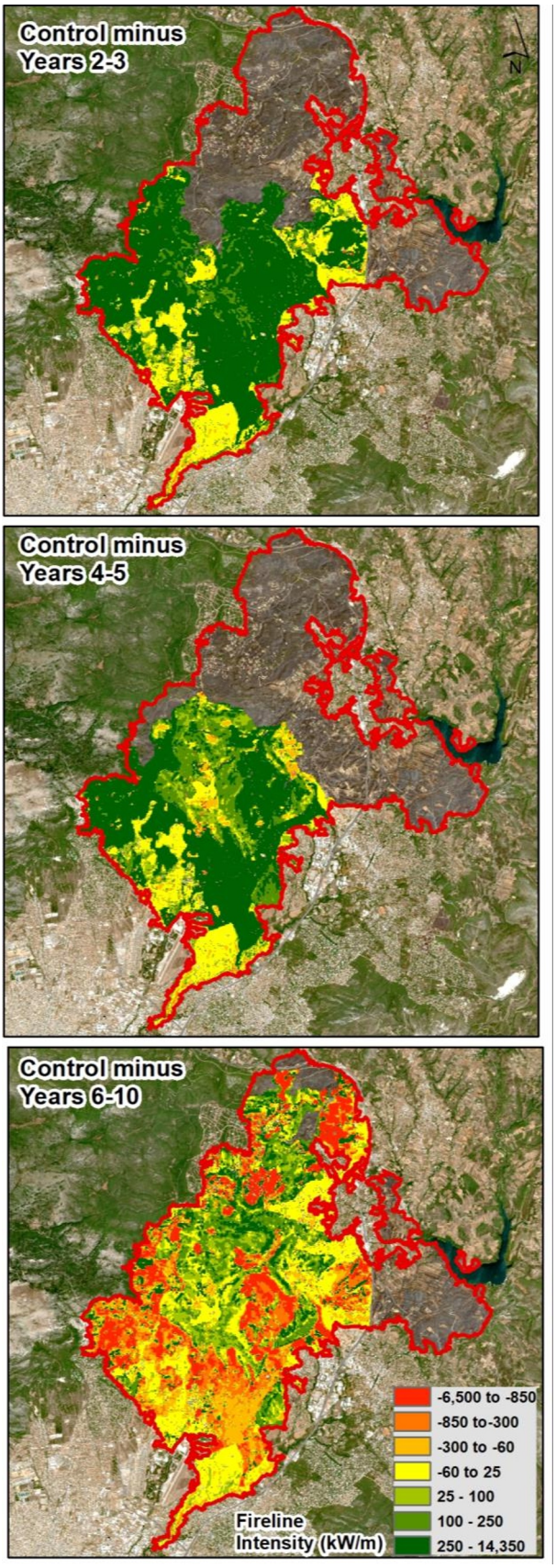

Fig. 9. Differences in fireline intensity (kw/m) after subtracting from the control simulation the results for the years 2-3, 4-5 and 6-10.

3.3 Differences in fire probabilities and fire intensity between 2021 and 2031

From the stochastic simulations of 10,000 fires for the two periods, we found that in the central and southern part of the burned area in 2021 an increase in the probability of burning is expected in the central and southern part of the burned area of 2021, estimated to result from changes in vegetation structure and composition in 2031 (Figure 9). This large increase suggests that the fires that will affect the area will be larger and more numerous than those simulated in 2021. However, it is a fact that the increase in burn probability does not correlate with changes in burn intensity (flame length). It is logical that in an area no longer dominated by overstory vegetation, but where the fuel is in the form of young coniferous or shrub stands, there should not be a large energy release which in the simulations is expressed in terms of flame length. It is found that in most of the study area, the flame length has almost no decrease or increase, but in some parts in the central and northern parts of the 2021 burned area there is a decrease, while in smaller parts there is an increase (Figure 10).

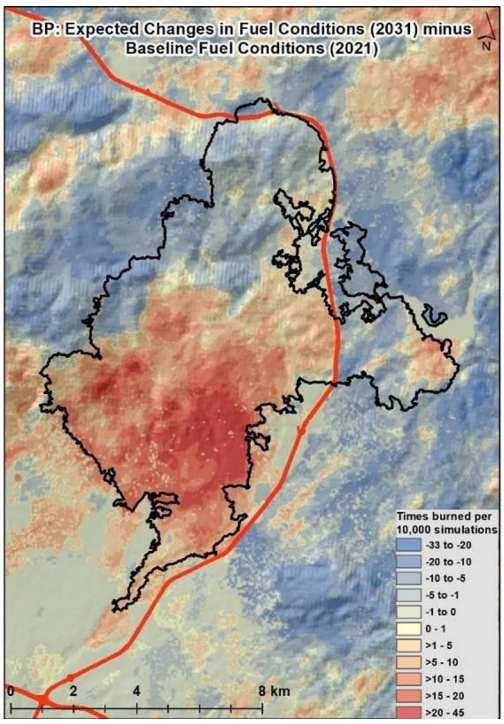

Fig. 10. Differences in the probability of an area burning (times that each pixel can burn per 10,000 fire simulations) after applying changes in surface and canopy fuel status between 2031-2021. Positive values (warmer colors) indicate an increase in 2031, while negative values (cooler colors) indicate a decrease relative to the 2021 conditions.

3 Discussion and Conclusions

In this study, we aimed to map burn severity and uncover wildfire spread patterns to enhance our understanding of fire behavior and provide valuable information for wildfire management strategies. By

employing remote sensing techniques and spatial analysis, we analyzed the burn severity and spatial patterns of wildfire spread within a specific region. The findings from this research contribute to the broader field of fire ecology and provide insights into the complex dynamics of wildfires.

The above raises the question of how the settlements, the infrastructure, the natural and cultural heritage monuments, but most importantly, the forest ecosystem and the natural environment of the region could have been protected from the fire of August 3rd, 2021, but also how they could be affected by possible future fires. The problem of forest fire spread within urban areas in these municipalities is complex and factors such as vegetation type, continuity and density, topography, the layout of buildings on the site, the potential existence of fuel management projects, and local meteorological parameters interplay in various combinations and will continue to play a significant role in the exposure of each settlement or infrastructure.

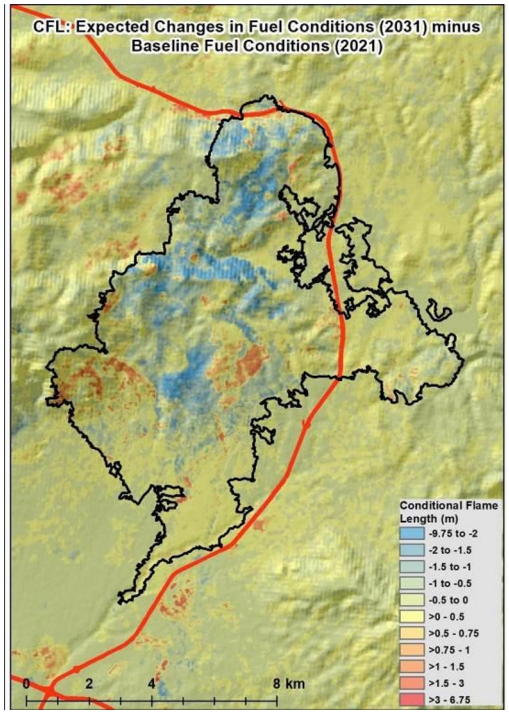

Fig. 11. Differences in flame length between the two periods in meters, after applying changes in surface and canopy fuel status between 2031-2021. Positive values (warmer colors) indicate an increase in 2031, while negative values (cooler colors) indicate a decrease compared to the 2021 conditions.

Our analysis of burn severity revealed distinct spatial patterns within the study area. We identified three burn severity classes: low, moderate, and high. The low severity areas were primarily characterized by minimal damage to vegetation, with the fire mostly confined to the forest floor. Moderate severity areas exhibited a higher level of vegetation damage, including partial tree mortality. High severity areas experienced extensive vegetation loss, with complete tree mortality and significant impact on the ecosystem. Understanding the distribution and extent of burn severity is crucial for prioritizing post-fire management efforts, such as reforestation and habitat restoration (Figure 11).

Fig. 12. Conifer seedlings mixed with annuals and short shrubs, forming a dense horizontal layer of live fuels mixed with dead branches from the burned forest.

Furthermore, our investigation into wildfire spread patterns revealed important insights into the dynamics of fire propagation. We utilized wildfire simulations to examine the direction and speed of fire spread. Our results indicated a predominant uphill spread pattern, with wildfires moving in the opposite direction of the prevailing wind. This finding emphasizes the critical role of topography in influencing fire behavior and highlights the importance of considering not only wind patterns, but also topography when developing fire management strategies. This information can be used to better allocate fuel management projects and establish effective firebreaks.

Moreover, our study demonstrated the value of remote sensing techniques for mapping burn severity and analyzing fire spread patterns. The utilization of satellite imagery, combined with advanced spatial analysis, enabled us to obtain accurate information about wildfire impacts. Remote sensing provides a cost-effective and efficient means of assessing burn severity over large areas, which is crucial for supporting decision-making processes in wildfire management. The integration of remote sensing data with other geospatial information, such as topography and weather patterns, can further enhance our understanding of fire behavior and aid in the development of predictive models.

In conclusion, this study contributes to the growing body of knowledge on burn severity mapping and wildfire spread patterns. The identification of distinct burn severity classes and the analysis of fire spread dynamics provide valuable information for land managers and decision-makers. By understanding the spatial patterns of burn severity and the factors influencing fire propagation, we can develop more targeted and effective strategies for wildfire management, including post-fire rehabilitation and prevention measures. The utilization of remote sensing techniques and spatial analysis tools offers a promising approach to enhance our understanding of fire ecology and support evidence-based decision-making in wildfire-prone regions. Future research should focus on refining

predictive models that incorporate various factors affecting burn severity and fire spread, ultimately leading to more effective and efficient wildfire management practices.

Fig. 13. Regeneration in the burned area, two years post-fire.

This study was funded by VIANEX SA, GlaxoSmithKline S.A., Groupama S.A, Rossi S.A. through the research initiative Varibopi-Reset.

References

1. M. Athanasiou, G. Xanthopoulos, *In the proceedings of the 14th Panhellenic Forestry Conference* (Patras, Greece, 2009)
2. M. Athanasiou, G. Xanthopoulos, *In the Proceedings of the 17th Panhellenic Forestry Conference* (Argostoli, Kefalonia, 2015)
3. M. Athanasiou, G. Xanthopoulos, *In the proceedings of the 20th Panhellenic Forestry Conference* (Trikala, Greece, 2021)
4. D.C. Lutes, R. E. Keane, J.F. Caratti, C.H. Key, N. H. Benson, S. Sutherland, L. J. Gangi, *FIREMON: Fire effects monitoring and inventory system* (Fort Collins, CO, USDA Forest Service, Rocky Mountain Research Station 2006)
5. M.A. Finney, *Farsite: Fire Area Simulator – Model Development and Evaluation* (Missoula, MT, USDA Forest Service, Rocky Mountain Research Station 2004).
6. J.H. Scott, R.E. Burgan, *Standard Fire Behavior Fuel Models: A Comprehensive Set for Use with Rothermel's Surface Fire Spread Model* (Fort Collins, CO, USDA Forest Service, Rocky Mountain Research Station 2005)